Proceedings of the 1999 IEEE
International Conference on Robotics & Automation
Detroit, Michigan • May 1999

Making Feasible Walking Motion of Humanoid Robots From Human Motion Capture Data

Anirvan DASGUPTA Yoshihiko NAKAMURA

Department of Mechano-Informatics,
University of Tokyo,
7-3-1 Hongo, Bunkyo-ku, Tokyo 113.

Abstract

This work presents a study of the human / humanoid locomotion system, and a method for adaptation of the Human Motion Capture Data *(HMCD) for driving a humanoid robot. The analysis uses the previously defined concept of the* Zero Moment Point *(ZMP) which provides a basis for the adaptation of the HMCD. An appropriate model of the robot foot, in agreement with the HMCD, is proposed. This model is used to plan a desired ZMP trajectory. A scheme for approximately matching the actual ZMP trajectory to the desired ZMP trajectory, through periodic joint motion correction at selected joints, is discussed. A method for resolving the ground reaction forces at the foot is also proposed.*

1 Introduction

Research on walking machines in general and biped robots in particular has been an active area of research in robotics (see [1], [2], [3], [4]). However, research on humanoid robots presents a number of new and exciting challenges to the existing research. One of the important problems of research on humanoid robots is that of imparting human-like locomotion capabilities to the humanoid. To accomplish this, it is quite natural to attempt using the HMCD to drive the robot. However, careful analysis reveals that the the HMCD cannot be used directly for a humanoid robot because of kinematic and dynamic inconsistencies between the human subject (whose motion is recorded) and the humanoid. Further, humans and the humanoid robots are underactuated systems with no actuation between the foot and the ground. The kinematic inconsistency requires kinematic corrections while calculating the joint angle trajectory. However, the dynamic inconsistency and the problem of underactuation requires a more careful study for controlling such a system. This paper focuses on the this aspect of the problem.

Vukobratovic *et. al* [1] studied the stability of biped gaits and proposed the the concept of Zero Moment Point (ZMP). A control theoretic formulation of the biped robot dynamics using the singular perturbation theory was presented by Miyazaki and Arimoto [3]. Furusho and Masubuchi [5] proposed a reduced order model for studying the stability and control of biped robots. They used a linearized model about the equilibrium point of a foot-less five-link biped robot. Li *et. al* [6] suggested the use of upper body motion correction for stabilizing a biped robot. They also used linearization and decoupling of the biped robot model. Fujimoto and Kawamura [9] proposed a hybrid position-force control based approach to control of biped robots.

Most of the previous research works on biped locomotion assumes a functional form, or uses an appropriate oscillator to generate the joint angle motions. Further, they consider a flat landing and take-off of the robot foot instead of a more natural and smooth *rolling*-like motion of the human foot. In this paper, we use the human motion capture data to generate human-like walking motions for the humanoid. To obtain the HMCD, markers are attached to a human subject at the limbs and joints, and the walking motion is captured simultaneously from many angles. This was performed using the VICON-370 system from Oxford Metrics. The recorded data is processed to obtain the cartesian coordinates of the markers from which the joint angles can be easily calculated using the kinematic model of the human subject. Due to the presence of underactuation, the human motion data cannot be used directly to drive the humanoid. Using the concept of ZMP, an approach to make feasible walking motion for humanoid robots has been presented. The proposed approach considers complete non-linear inverse dynamics model of the humanoid. A suitable modeling of the robot foot has been proposed in agreement with the human motion data. Finally, an approach to compute the foot forces is also presented.

2 The ZMP and its significance

The humanoid robot, being an underactuated mechanism, cannot directly reproduce the motion as in the

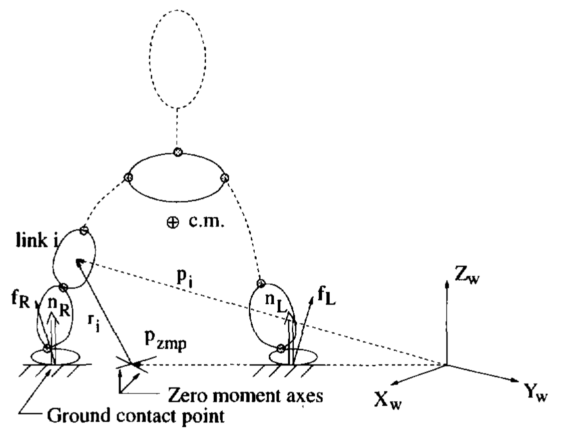

Figure 1: Definition of ZMP for a kinematic chain

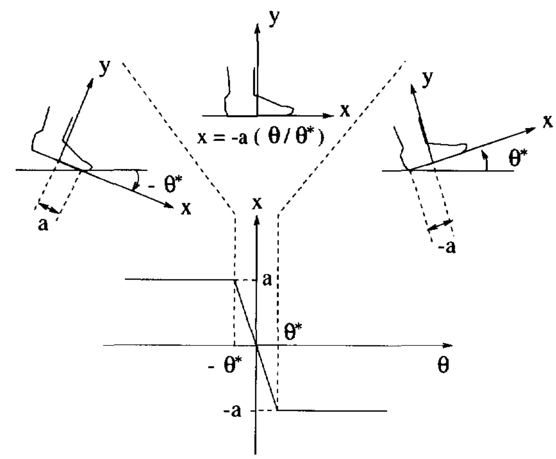

Figure 2: Model of the robot foot

HMCD. Hence, the first step is to identify and characterize the set of feasible motions of the robot. This is done on the basis of the ZMP. The concept of ZMP was proposed by Vukobratovic [1] to study the stability of biped robots. The ZMP is defined as that point on the ground at which the net moment of the inertial forces and the gravity forces has no component along the horizontal axes. For the kinematic chain as shown in Fig. 1, the ZMP condition can be represented as

$$\sum_i (\mathbf{r}_i \times m_i\mathbf{a}_i + \mathbf{I}_i\boldsymbol{\alpha}_i + \boldsymbol{\omega}_i \times \mathbf{I}_i\boldsymbol{\omega}_i) - \sum_i \mathbf{r}_i \times m_i\mathbf{g} = (0,0,*)^T \tag{1}$$

where, $\mathbf{r}_i = \mathbf{p}_i - \mathbf{p}_{zmp}$, m_i and $\mathbf{I}_i$ are, respectively, the mass and moment of inertia of the i^{th} link, $\boldsymbol{\omega}_i$ and $\boldsymbol{\alpha}_i$ are, respectively, the angular velocity and angular acceleration of the i^{th} link, and $\mathbf{g}$ is the acceleration due to gravity. All the quantities in (1) are known (from the knowledge of the inertial parameters, and the HMCD) except $\mathbf{p}_{zmp}$. However, $\mathbf{p}_{zmp} = (x_{zmp}, y_{zmp}, 0)^T$. Thus, there are two unknowns, and (1) will provide two independent equations from which $\mathbf{p}_{zmp}$ can be solved.

The *ground contact point* of a foot is defined as the point on the foot through which a resultant reaction force, and a reaction moment, orthogonal to the ground surface, acts (see Fig 1). Using this definition, the rate of change of moment of momentum of the whole system about the ZMP, in the two-leg support phase, can be written as

$$-\sum_i (\mathbf{r}_i \times m_i(\mathbf{a}_i - \mathbf{g}) + \mathbf{I}_i\boldsymbol{\alpha}_i + \boldsymbol{\omega}_i \times \mathbf{I}_i\boldsymbol{\omega}_i) + \mathbf{r}_L \times \mathbf{f}_L + \mathbf{r}_R \times \mathbf{f}_R + \mathbf{n}_L + \mathbf{n}_R = 0 \tag{2}$$

where, $\mathbf{r}_{L/R} = \mathbf{p}_{L/R} - \mathbf{p}_{zmp}$, $\mathbf{p}_{L/R}$ is the position of the left/right foot contact point, and $\mathbf{f}_{L/R}$ and $\mathbf{n}_{L/R}$ represents, respectively, the ground reaction force and moment at the left/right foot. The vector $\mathbf{r}_{L/R}$ is of the form $(*,*,0)^T$ while, $\mathbf{n}_{L/R}$ is of the form $(0,0,*)^T$. Using (1) in (2), we have

$$\mathbf{r}_L \times \mathbf{f}_L + \mathbf{r}_R \times \mathbf{f}_R + \mathbf{n}_L + \mathbf{n}_R = (0,0,*)^T. \tag{3}$$

It may be observed from (3) that, for a feasible motion, the ZMP must always lie within the foot-print polygon. However, using the HMCD for the humanoid, it was observed that the the ZMP does not satisfy this condition. Hence, the HMCD needs to be corrected to satisfy this basic feasibility condition.

3 Adaptation of the HMCD for nonlinear dynamic model of humanoid

The adaptation of the HMCD for the humanoid robot consists of two steps. First, we set a desired ZMP trajectory based on the foot motion data in the HMCD. For this, we propose to model the motion of the human foot appropriately as discussed in Sec. 3.1. Next, we use periodic joint motion corrections at selected joints to approximately match the desired ZMP trajectory.

3.1 Modeling of the foot

The HMCD reveals that the human foot exhibits a *rolling*-like motion on the ground. The foot lands on the heels, gradually rolls onto the face of the foot, and finally the contact moves to the toe before it is lifted. This motion is modeled as illustrated through Fig. 2. Using the foot orientation and the piecewise-linear function as shown in Fig. 2, the ground contact point of the foot can be located. The piecewise-linear function is set based on the dimensions of the foot. The coordinates of the ground contact point obtained thus will be necessary for setting a desired ZMP trajectory, and also for calculating the foot forces as will be discussed in Sec. 4. As

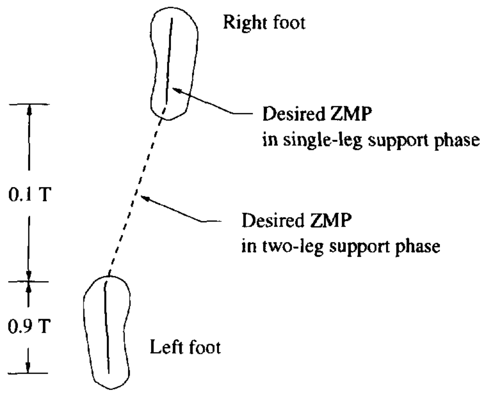

Figure 3: Setting of the desired ZMP trajectory

is evident, the proposed model allows a smooth motion of the ground contact point over the face of the foot.

3.2 Setting of desired ZMP trajectory

During the single-leg support phase, the ground contact point obtained from the foot model of Sec. 3.1 is taken as the desired ZMP. During the two-leg support phase, the desired ZMP is set by linearly interpolating between the ground contact points of the two legs. This is illustrated through Fig. 3. It is observed from the HMCD that the time interval for the two-leg support phase is much smaller than the single-leg support phase. Since the stride-length is much longer than the foot length, the average speed of the ZMP in the two-leg support phase is much higher than in the single-leg support phase. Hence, the desired ZMP trajectory possesses spatial and temporal characteristics. This implies that a simple sinusoidal curve, as is considered in [6], cannot appropriately represent a desired ZMP trajectory. Thus, the proposed method of generating the desired ZMP trajectory is important to preserve the naturality of the walking motion.

3.3 Optimization problem for ZMP matching

Since the ZMP is a point on the two dimensional ground surface, we can control its trajectory by controlling the motion of two orthogonal joints with horizontal axes. For example, the simplest choice of two such joints are the waist joints as shown in Fig. 4. This choice is primarily motivated by the research reported in [6]. It is known that periodic motions are most appropriate for trajectory planning and control of underactuated mechanisms (see [7]). Moreover, since human locomotion is an almost periodic process, it is desirable to have this characteristic in the robot locomotion for naturality. Hence, any correction of the HMCD is to be achieved using only periodic signals. Since finite energy periodic signals can be represented through the *sine* and *cosine* functions (*i.e.* Fourier series), we represent the corrective motions in the form

$$\delta\theta_i = \sum_n a_{in} \sin n\omega_{wi}t + b_{in} \cos n\omega_{wi}t \tag{4}$$

where, $\delta\theta_i$ is the corrective motion at i^{th} joint, a_{in}, b_{in} represent the amplitude, and ω_{wi} is the frequency of the corrective motion. The ZMP, being a point on the ground plane, has two degrees of freedom. However, the Fourier expansion of the corrective signals may involve a large number of unknown coefficients. This allows us to formulate an optimization problem to determine the unknown coefficients for obtaining a good match between the actual and the desired ZMP trajectories as follows

$$Minimize \quad \mathcal{J} = \int ||\mathbf{p}_{zmp} - \mathbf{p}^d_{zmp}||^2 dt \tag{5}$$

where, $\mathbf{p}^d_{zmp}$ represents the desired ZMP trajectory. The above optimization problem involves the non-linear dynamics of the humanoid through the calculation of $\mathbf{p}_{zmp}$. The adaptation of the HMCD must also take into account the ground reaction forces at the feet. Any change in the HMCD will also change the ground reaction forces and may lead to slippage at the foot. Further, calculation of the joint torques using the inverse dynamics requires the foot reaction forces. Therefore, a procedure to calculate the ground reaction forces is outlined next.

4 Ground reaction force calculation

The equation of motion of the center of mass of the humanoid can be written as

$$m_{cm}\mathbf{a}_{cm} = \mathbf{f}_L + \mathbf{f}_R + m_{cm}\mathbf{g} \tag{6}$$

where, m_{cm} and $\mathbf{a}_{cm}$ are, respectively, the mass of the robot and the acceleration of the center of mass. During the single-leg support phase, the foot force is obtained directly from (6) as one of $\mathbf{f}_L$ or $\mathbf{f}_R$ will be zero. However, during the two-leg support phase, only the sum $\mathbf{f}_L + \mathbf{f}_R$ is known, and hence, has to be resolved appropriately to minimize the internal force. Methods for resolving the leg reaction forces was considered in [10] and [11]. However, their methods do not consider the motion of the ground contact point on the surface of the foot. Further, smooth transition of the forces during placement and take-off is not be ensured.

During the two-leg support phase, the z-component (vertical) of the force is determined from the first two equations in (3)

$$\begin{aligned} y_L f_{L3} + y_R f_{R3} &= y_{zmp}(f_{L3} + f_{R3}) \qquad (7)\\ x_L f_{L3} + x_R f_{R3} &= x_{zmp}(f_{L3} + f_{R3}) \qquad (8) \end{aligned}$$

where, $x_{L/R}$ and $y_{L/R}$ are, respectively, the x and y coordinates of the foot contact points in the world coordinate frame, and $f_{L/R3}$ represents the foot contact force component along the z coordinate (vertical) direction. The coordinates $x_{L/R}$ and $y_{L/R}$ in the two-leg support phase are estimated from the foot contact model of Sec. 3.1. The term $(f_{L3} + f_{R3})$ on the right hand side of (7)-(8) is known from the third equation in (6). The tangential force components in the two-leg support phase is resolved based on the following requirements namely, (a) the leg forces must satisfy (6), (b) the friction constraint must be satisfied at each ground contact point, and (c) the internal force in the closed-loop structure must be minimum. For this purpose, the following linear programming problem (LPP) is formulated.

$$
\begin{aligned}
&Min && -d_1 - d_2 && (9)\\
&subject\ to && f_{L1} + f_{R1} = m_{cm}a_{cm1} && (10)\\
& && f_{L2} + f_{R2} = m_{cm}a_{cm2} && (11)\\
& && \mathbf{P}[f_{L1}, f_{L2}, f_{R1}, f_{R2}]^T + d_1\mathbf{1} < \mathbf{b} && (12)\\
& && \frac{(\mathbf{p}_L - \mathbf{p}_R)^T}{\|\mathbf{p}_L - \mathbf{p}_R\|}(\mathbf{f}_L - \mathbf{f}_R) + d_2 < 0 && (13)\\
& && \frac{-(\mathbf{p}_L - \mathbf{p}_R)^T}{\|\mathbf{p}_L - \mathbf{p}_R\|}(\mathbf{f}_L - \mathbf{f}_R) + d_2 < 0 && (14)\\
& && d_1,\ d_2 > 0 && (15)
\end{aligned}
$$

where,

$$
\mathbf{P} = \begin{bmatrix} 1 & 0 & 0 & 0 \\ -1 & 0 & 0 & 0 \\ 0 & 1 & 0 & 0 \\ 0 & -1 & 0 & 0 \\ 0 & 0 & 1 & 0 \\ 0 & 0 & -1 & 0 \\ 0 & 0 & 0 & 1 \\ 0 & 0 & 0 & -1 \end{bmatrix} \quad \text{and } \mathbf{b} = \begin{bmatrix} -\mu f_{L3} \\ -\mu f_{L3} \\ -\mu f_{L3} \\ -\mu f_{L3} \\ -\mu f_{R3} \\ -\mu f_{R3} \\ -\mu f_{R3} \\ -\mu f_{R3} \end{bmatrix};
$$

μ is the coefficient of friction, and $\mathbf{1} = (1, \ldots, 1)^T$. The constraints (10) and (11) are obtained from the first two equations in (6), and (12) represents the linearized friction constraint and is formulated based on the work of Kerr and Roth [8]. The internal force constraints are given by (13)-(14). The scalar d_1 in (11) physically represents the contact stability margin, while the scalar d_2 in (13)-(14) is in inverse proportion to the internal force. Thus, by minimizing $(-d_1 - d_2)$, we obtain the ground reaction forces which maximizes the stability against sliding and minimizes the internal force during the two-leg support phase. The proposed scheme also ensures a smooth transition of the foot forces during its lift or placement.

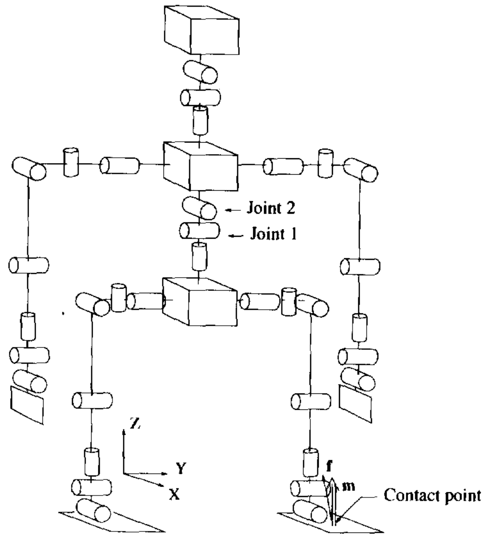

Figure 4: Kinematic model of the humanoid robot

Link	*Mass(kg)*	*MomentofInertia(kgm²)*
Pelvis	16.61	(0.23, 0.18, 0.16)
Trunk	29.27	(0.73, 0.63, 0.32)
Head	5.89	(0.03, 0.033, 0.023)
Arm	2.97	(0.025, 0.025, 0.005)
Forearm	1.21	(0.005, 0.0054, 0.0012)
Hand	0.55	(0.0016, 0.002, 0.0005)
Thigh	8.35	(0.15, 0.16, 0.025)
Shank	4.16	(0.055, 0.056, 0.007)
Foot	1.34	(0.0018, 0.0075, 0.007)

Table 1: Range of values for n_l, n_f, n_d, n_p and n_c

5 Numerical example

We consider a numerical example consisting of a 40 degrees of freedom humanoid model as shown in Fig. 4. The dynamic parameters of the model are presented in Tab. 1, where the moments of inertia are the principal moments about the center of mass of the links. The total walking time for nine steps is assumed to be 9.0 sec (about 2km/hr). The desired ZMP trajectory is shown in Fig. 5(a). It may be observed that the ZMP is clustered during the single leg support phase and relatively sparse during the two leg support phase. This is because the transition from one leg to another takes place very fast compared to the motion with single-leg support. On the other hand, the initial ZMP trajectory (as calculated from the HMCD) in Fig. 5(b) shows an almost uniform distribution of the ZMP over the trajectory. This is due to the combined effects of the difference in the inertial parameters between the human subject and the humanoid, and the effects of filtering of the HMCD.

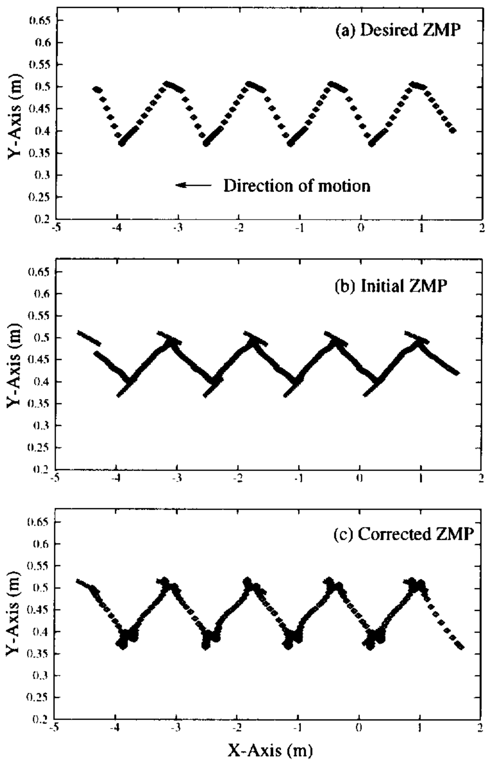

Figure 5: Desired, initial and corrected ZMP trajectories

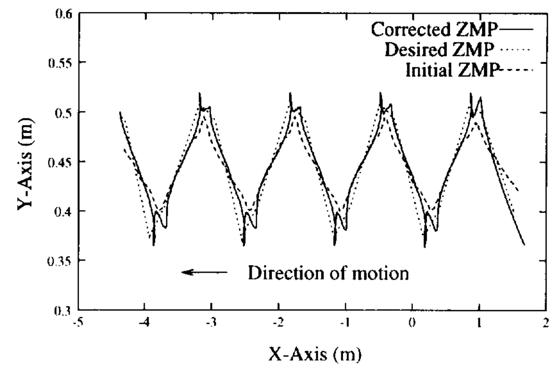

Figure 6: Comparison of spatial characteristics of desired, initial and corrected ZMP trajectories

Further, the shape (spatial characteristics) of the initial ZMP trajectory is not in match with the desired ZMP trajectory. Thus, not only the shape of the ZMP trajectory, but also the temporal distribution of the ZMP has to be matched with the desired ZMP trajectory. We consider the corrective motions at joints 1 and 2 shown in Fig. 4 of the form (4) with three frequency terms, *i.e.*, $n = 1, 3$. The frequency components of the desired ZMP trajectory are calculated, and for $i = 1, 2$, ω_{wi} in (4) are set as $\omega_{w1} = 0.88$ Hz and $\omega_{w2} = 0.44$ Hz. The unknown parameters a_{in} and b_{in}, $i = 1, 2$ and $n = 1, 3$ in (4) are determined by minimizing the objective function (5) using the steepest descent technique.

The spatial characteristics of the desired, initial and the corrected ZMP trajectories are compared in Fig. 6. Some oscillations are observed in the single-leg contact phases especially at the transition of the single-leg and two-leg support phases. Such oscillations (for example, the Gibbs phenomenon) are expected with the Fourier series in cases of sharp transition. The temporal distribution of the corrected ZMP trajectory, presented in Fig. 5(c), shows a fairly good match with Fig. 5(a). The foot, and the ZMP locations for the initial and corrected motions are shown in Fig. 7 at two instants namely, when the left foot is just placed, and subsequently the right foot is just lifted. It is observed from the figures that the ZMP condition is now satisfied after the correction of the motion.

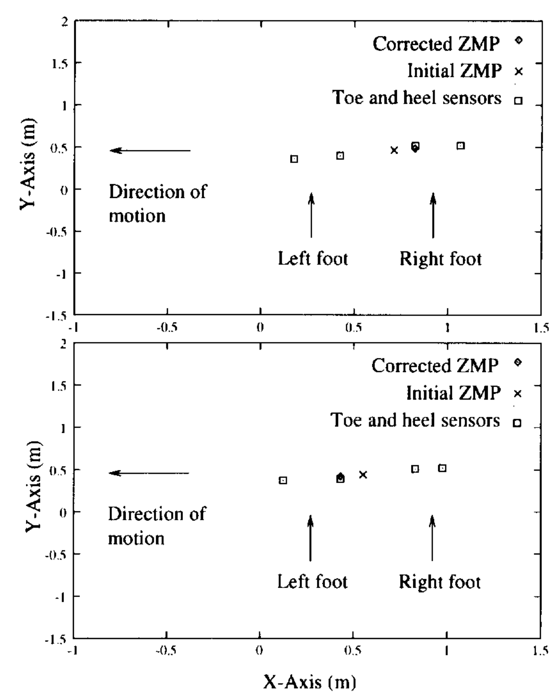

Figure 7: Feet and ZMP locations

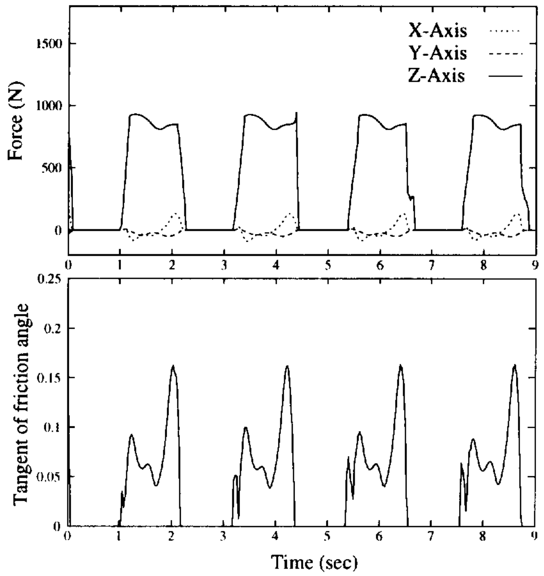

Figure 8: Left foot forces and the tangent of friction angle

Next, the ground reaction forces on the legs are resolved based on the discussion presented in Sec. 4. The reaction forces on the left foot and the tangent of the friction angle are plotted in Fig. 8 for the corrected motion. Once a feasible joint angle motion of the humanoid alongwith the foot forces are obtained, the joint torques can be easily calculated using the inverse dynamics equations.

6 Conclusions and future work

In this paper, we proposed a method of making feasible walking motion of humanoid robots from human motion capture data.

1. The feasibility of the walking data was characterized based on the concept of ZMP.

2. Using an appropriate model of the foot in agreement with the HMCD, the desired ZMP trajectory was generated.

3. Assuming periodic corrective motions represented in Fourier series, an optimization problem was formulated to determine the unknown coefficients of the Fourier series. The complete non-linear dynamics of the humanoid was considered in this optimization.

4. A method for calculating the ground reaction forces was proposed which enables one to calculate the joint torques for driving the humanoid using the inverse dynamics equations.

The next step will be to develop an appropriate control strategy for the system which will be tested through dynamic simulation.

Acknowledgement: The first author would like to gratefully acknowledge the financial support from the Ministry of Education (Monbusho), JAPAN. This work was supported by Humanoid Robotics Project, MITI, JAPAN.

References

[1] Vukobratovic, M., Frank, A.A., and Juricic, D., 1970, "*On the Stability of Biped Locomotion*," IEEE T. on Biomed. Engg., BME-17, No. 1, pp. 25-36.

[2] Golliday, C.L. Jr., and Hemami, H., 1977, "*An Approach to Analyzing Biped Locomotion Dynamics and Designing Robot Locomotion Controls*," IEEE T. on Auto. Control, Vol. AC-22, No. 6, pp. 963-972.

[3] Miyazaki, F., and Arimoto, S., 1980, "*A Control Theoretic Study on Dynamical Biped Locomotion*," T. of ASME, J. of Dyn. Sys. Meas. Control, Vol. 102, pp. 233-239.

[4] Morecki, A., and Waldron, K.J., Eds., 1997, "*Human and Machine Locomotion*," Springer-Verlag.

[5] Furusho, J., and Masubuchi, M., 1986, "*Control of a Dynamic Biped Locomotion System for Steady walking*," T. of ASME, J. of Dyn. Sys. Meas. and Cont., Vol. 108, pp. 111-118.

[6] Li, Q., Takanishi, A., and Kato, I., 1993, "*Learning Control of Compensative Trunk Motion for Biped Walking Robot based on ZMP Stability Criterion*," J. of the Rob. Soc. of Japan, Vol. 11, No. 4, pp. 77-83 (in Japanese).

[7] Suzuki, T., 1997, "*Analysis and Control of Nonholonomic Systems Under Dynamical Constraints*", Ph.D. Dissertation, Graduate School, Univ. of Tokyo.

[8] Kerr, J. and Roth, B., 1986, "*Analysis of Multifingered Hands*," Int. J. of Rob. Res., Vol. 4, No. 4, pp. 3-17.

[9] Fujimoto, Y., and Kawamura, A., 1996, "*Proposal of Biped Walking Control Based on Robust Hybrid Position-Force Control*," IEEE Int. Conf. on Rob. and Auto., pp. 2724-2730.

[10] Gardner, J.F., Srinivasan, K., and Waldron, K.J., 1990, "*A Solution for the Force Distribution Problem in Redundantly Actuated Closed Kinematic Chain*," Trans. of ASME, J. of Dyn. Sys. Meas. and Cont., Vol. 112, pp. 523-526.

[11] Chevallereau, C., and Perrin, B., 1998, "*Computed Torque Control Law Under Constraints for Single and Double Support Motion of Planar Biped Robot*," 4^{th} ECPD Int. Conf. on Advanced Rob, Intelligent Automation and Active Systems, Moscow, pp. 214-219.